

Maximizing Transmission Capacity in Optical Communication Systems Utilizing Microresonator Comb Laser Source with Adaptive Modulation and Bandwidth Allocation Strategies

JUN HU,^{1,2†} WEI WANG^{3,4†}, ZHENYU XIE^{5†}, CHENGNIAN LIU^{1,2}, FAN LI^{3,4,*}, AND DAQUAN YANG^{1,2,*}

¹State Key Laboratory of Information Photonics and Optical Communications, Beijing University of Posts and Telecommunications, Beijing 100876, China

²School of Information and Communication Engineering, Beijing University of Posts and Telecommunications, Beijing 100876, China

³School of Electronics and Information Technology, Sun Yat-Sen University, Guangzhou 510275, China

⁴Key Laboratory of Optoelectronic Materials and Technologies, School of Electronics and Information Technology, Sun Yat-Sen University, Guangzhou 510275, China

⁵State Key Laboratory for Artificial Microstructure and Mesoscopic Physics and Frontiers Science Center for Nano-optoelectronics, School of Physics, Peking University, Beijing 100871, China

[†]These authors contributed equally to this work.

*ydq@bupt.edu.cn

*lifan39@mail.sysu.edu.cn

Compiled September 27, 2024

Traditional optical communication systems employ bulky laser arrays that lack coherence and are prone to severe frequency drift. Dissipative Kerr soliton microcombs offer numerous evenly spaced optical carriers with high Optical Signal-to-Noise Ratio (OSNR) and coherence in chip-scale packages, potentially addressing the limitations of traditional Wavelength Division Multiplexing (WDM) sources. However, soliton microcombs exhibit inhomogeneous OSNR and linewidth distributions across the spectra, leading to variable communication performance under uniform modulation schemes. Here, we demonstrate, for the first time, the application of adaptive modulation and bandwidth allocation strategies in Optical Frequency Comb (OFC) communication systems to optimize modulation schemes based on OSNR, linewidth, and channel bandwidth, thereby maximizing capacity. Experimental verification demonstrates that the method enhances spectral efficiency from 1.6 bit/s/Hz to 2.31 bit/s/Hz, signifying a 44.58% augmentation. Using a single soliton microcomb as the light source, we achieve a maximum communication capacity of 10.68 Tbps after 40 km of transmission in the C-band, with the maximum single-channel capacity reaching 432 Gbps. The projected combined transmission capacity for the C and L bands could surpass 20 Tbps. The proposed strategies demonstrate promising potential of utilizing soliton microcombs as future light sources in next-generation optical communication.

<http://dx.doi.org/10.1364/ao.XX.XXXXXX>

1. INTRODUCTION

On the verge of information explosion, driven by the exponential growth of cloud applications and Internet traffic, ultra-high speed and capacity are demanded in optical fiber communications. Massively parallel Wavelength Division Multiplexing (WDM) is deemed crucial for achieving ultra-high capacity in optical communications [1–6]. However, conventional commercial WDM systems, requiring tens or hundreds of lasers to provide optical carriers, significantly impact the size, cost, and power consumption of the system negatively [7–9]. The need for higher coherence and frequency stability of the carrier laser increases

with narrower channel spacing and higher data rates [10–12]. Practically, WDM systems require widened guard bands to prevent spectral overlap due to laser frequency offsets, which restricts the system's capacity from reaching the Shannon limit. Additionally, since the laser linewidth affects the phase noise of the signal, a broader linewidth results in greater phase fluctuations. These phase fluctuations cause demodulation errors, thereby degrading the performance of the transmission system, especially in higher-order modulation schemes[13]. However, the linewidths of Integrated Tunable Laser Arrays (ITLAs) in conventional WDM systems, typically several hundred kHz,

restrict their use in advanced modulation formats. A viable solution to this challenge is the adoption of Optical Frequency Comb (OFC) [14]. By pumping a Whispering-Gallery-Mode (WGM) microresonator with a continuous-wave laser, numerous OFCs with high-frequency stability and ultralow phase noise can be produced. Many types of resonators, including microring[15, 16], microdisk[17], and microsphere resonators[18], are capable of generating OFC.

Silicon nitride (Si_3N_4) microring resonators, compared to other types, offer a more mature process for generating broadband and fully phase-coherent time-dissipative Kerr solitons (DKS), presenting significant potential as on-chip optical frequency comb generators. Recently, OFCs have found extensive applications in fields like sensing[19–22], timekeeping[23, 24], spectroscopy[25], precision metrology[26, 27], and optical communications[28–33]. In optical communications, OFCs have achieved significant advancements in capacity[30] and Digital Signal Processing (DSP) simplification[31]. However, as predetermined by the solution to the Lugiato-Lefever equation and the effect of repetition rate fluctuations, the Optical Signal-to-Noise Ratios (OSNRs) and linewidths of the soliton microcombs are not uniformly distributed[34, 35]. Therefore, using one fixed modulation scheme will inevitably fail to effectively utilize the full bandwidth potential of soliton microcombs. Among the conventional communication algorithms[36, 37], adaptive modulation and bandwidth allocation strategies stand out as promising solutions. Adaptive modulation dynamically adjusts the modulation scheme by continuously monitoring the Channel State Information (CSI), selecting the modulation that best suits the current environment to optimize the data transmission rate and reliability. Bandwidth allocation strategies dynamically distribute bandwidth resources in a communication network and adjust bandwidth in real time based on changes in network traffic to improve resource utilization.

Here, we introduce the use of adaptive modulation and bandwidth allocation strategies for the first time in high-capacity OFC communication experiments. Unlike conventional commu-

nication systems that dynamically adjust based on CSI and user resources, this study applies strategies to optimize symbol rates and modulation formats for comb lines with varying carrier qualities (e.g., OSNR, linewidth), to enhance spectral efficiency and communication quality. For comb lines with lower communication performance, in this paper, the unused bandwidth in the channel is effectively utilized by converting the bandwidth space in the frequency domain to the phase space in the constellation diagram, using a low-order modulation format and a high-speed symbol transmission rate. This approach results in a 44.58% improvement in spectral efficiency. In addition, the adaptive modulation and bandwidth allocation strategy optimizes the system communication capacity based on OFC quality and system resources. Therefore, it is applicable to all OFC communication systems. With this method, we experimentally measure the capacity limit of each channel in a single soliton microcomb generated by a Si_3N_4 microring resonator. The system utilizes 39 optical combs in the C-band, achieving a total transmission capacity of 10.68 Tbps over a distance of 40 km, with a maximum single-channel capacity of 432 Gbps. This exceeds the single-channel capacity of the next-generation commercial WDM system of 400 Gbps. Additionally, we present the experimentally measured single-sideband (SSB) frequency noise for each channel of the soliton microcomb. The frequency noise is minimal near the pump light and increases continuously toward both ends, with the minimum measured frequency noise being $17.56\text{Hz}^2/\text{Hz}$, equivalent to a Lorentzian linewidth of 107 Hz. The experimental results demonstrate that the communication quality of different comb lines in a soliton microcomb mainly depends on the OSNR and linewidth of individual comb lines. The communication capacity of the soliton microcomb can be maximized by using adaptive modulation algorithms and bandwidth allocation strategies dynamically adjusted according to the conditions of each channel.

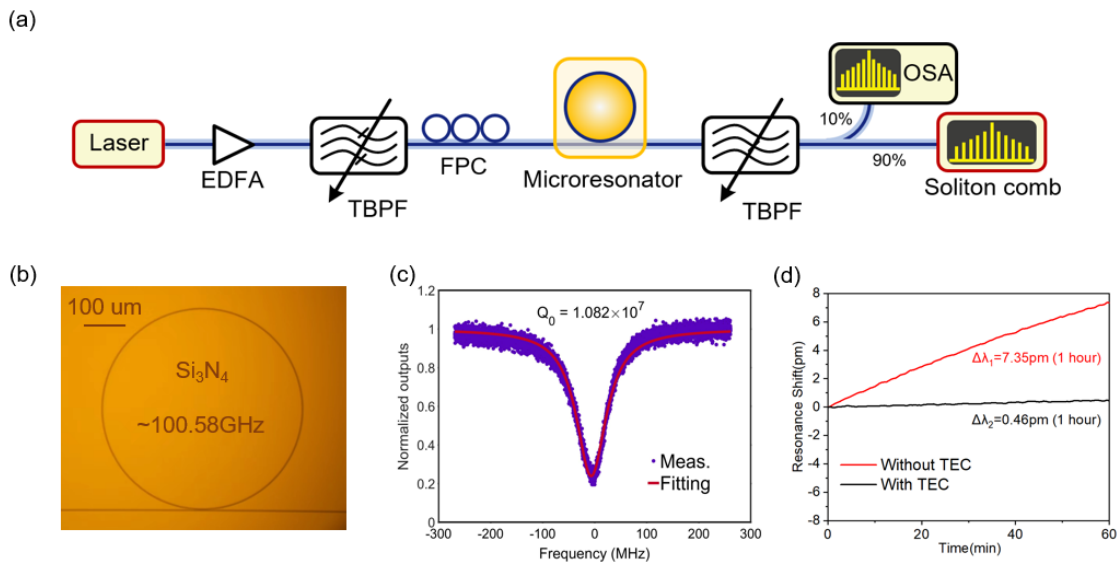


Fig. 1. (a) Experimental setup for generating a single soliton microcomb in a high-Q Si_3N_4 microring resonator. EDFA: Erbium-Doped Fiber Amplifier; TBPF: Tunable Bandpass Filter; FPC: Fiber Polarization Controller; OSA: Optical spectrum Analyzer. (b) Microscope photo of a Si_3N_4 microring resonator with a radius of about 240 μm . (c) Typical transmission spectrum and Q-factor of the resonator resonance mode. (d) Variation of one hour resonance wavelength with and without temperature control.

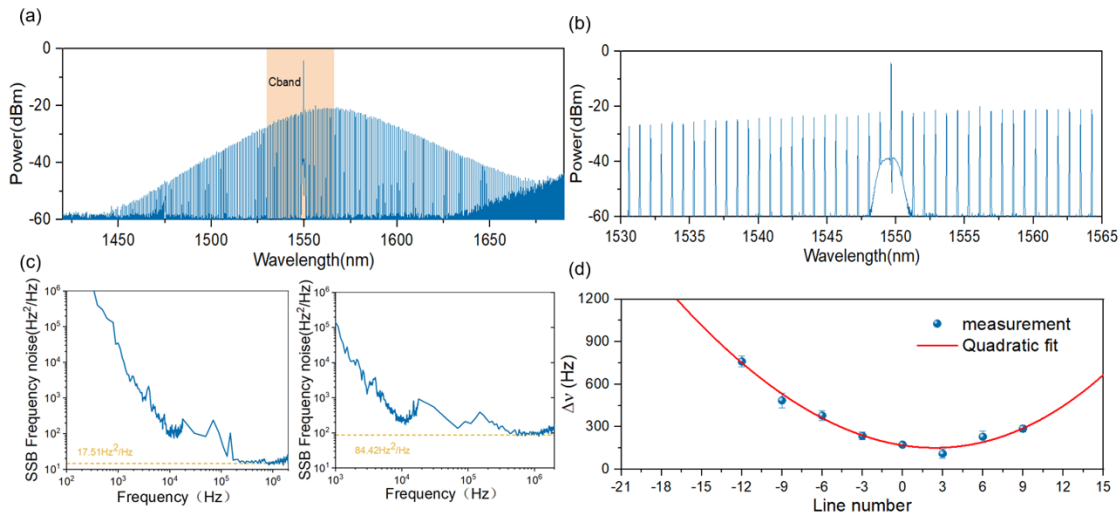


Fig. 2. (a) Optical spectra of the single soliton microcomb. (b) C-band spectra of the single soliton microcomb before modulation. (c) The respective SSB frequency noise spectra of the 1552nm and 1542.4nm comb line. (d) The distribution of the soliton microcomb linewidth. The error bar stands for the standard deviation of three measurements.

2. GENERATION AND CHARACTERIZATION OF THE SINGLE SOLITON MICROCOMB

Before conducting the soliton microcomb communication experiments to verify the effects of adaptive modulation and bandwidth allocation strategies, we first measure the OSNR and linewidth of the soliton microcomb. Fig. 1(a) illustrates the experimental setup used to generate a soliton microcomb in a high-Q Si_3N_4 microring resonator. This setup facilitates the generation of a stable soliton microcomb using minimal instrumentation and straightforward operation, maintaining stability for over 10 hours. In coherent optical communications, the Lorentz linewidth is critical as it controls the instantaneous frequency and phase fluctuations over short time scales, requiring precise tracking by receivers to effectively compensate for distortion. Dissipative solitons demonstrate low-noise coherent states, with the ideal scenario being that the frequency noise of the soliton microcomb is primarily derived from the pump laser's frequency noise. Consequently, an ultra-narrow linewidth fiber laser is used as the pump source. While lower-power pump light can generate stable soliton microcomb, amplifying the narrow linewidth laser to about 26 dBm using an Erbium-Doped Fiber Amplifier (EDFA) optimizes the OSNR of the carrier. However, the Amplified Spontaneous Emission (ASE) noise from the EDFA reduces the OSNR of carriers near the pump light, requiring a narrowband bandpass filter post-EDFA to mitigate ASE noise. Optimal optical power distribution occurs when the polarization of the Continuous-Wave (CW) pump laser aligns with its polarization axis. To achieve this, polarization controllers are used to adjust the polarization state. A Fiber Bragg Grating (FBG) is employed post-packaging of the Si_3N_4 microresonator to suppress the residual pump light.

The transmission power spectrum is recorded by a photodetector and monitored by an oscilloscope, while the soliton spectrum is monitored by a spectrometer. Fig. 1(b) displays a microscope photo of the packaged Si_3N_4 microring resonator used for communication experiments, with a free spectral range (FSR) of approximately 100.58 GHz and enclosed with a temperature sensing control module for temperature stabilization. Fig. 1(c) shows the Q factor of the Si_3N_4 microring resonator with an

intrinsic Q of 1.082×10^7 . To assess the long-term stability of the sensing system, the shifts of the resonance wavelength with and without temperature control are measured over time. The resonant frequency shift with temperature control, as shown in Fig. 1(d), is suppressed by an order of magnitude to a mere 0.46 pm, indicating outstanding stability of the packaging. Additionally, the generated soliton microcomb can also be maintained for more than 10 hours, showing great potential in long term operation.

After suppressing the residual pump light, the measured spectrum of the single soliton microcomb is shown in Fig. 2(a), exhibiting a smooth spectrum profile with a 3 dB bandwidth of 6 THz. The soliton microcomb features a broad spectrum in the frequency domain, which generates ultra-high power pulsed signals in the time domain. Meticulous power management is crucial to protect the In-phase and Quadrature Modulator (IQM) from potential damage caused by excessive comb power. Additionally, since C-band fiber has the lowest transmission loss and is the most commonly used band in WDM systems, which are widely used in Metropolitan Area Networks (MAN), long-haul, ultra-long-haul, and submarine fiber cable systems, our experiments also focus on the C-band region. Fig. 2(b) shows the spectra of the soliton microcomb within the C-band region. A 10 dB difference in comb line power can be observed, which would affect the communication bandwidth if not addressed.

In addition, different communication modulation formats have different linewidth requirements for the optical carrier. In conventional communication systems, higher-order modulation formats increase the bandwidth for a given modulation rate, but require lower phase noise in the carrier to maximize constellation density in phase space. Employing an ultra-low noise pump laser allows the soliton microcomb to achieve extremely narrow linewidths. The gain of the soliton microcomb is based on resonantly enhanced continuous-wave pump parametric amplification, with noise induced by spontaneous scattering being extremely weak. Within the microcomb, the pump laser is coherently integrated into the comb-like spectrum, resulting in its noise being expected to be equally transferred to all comb lines. Previous studies have indicated that when the microcomb

operates with low noise, the comb lines inherit the linewidth of the pump, and farther lines attenuate more due to repetition noise within the cavity[35, 38].

The linewidth and OSNR of optical combs in coherent communication systems affect the communication capability of the system jointly. Here, a Delayed Self-Heterodyne Interference (DSHI) scheme is utilized[39] to measure the distribution of the soliton microcomb frequency noise. This method utilizes a laser to generate two light beams with different delays for self-heterodyning and exploits the spectral characteristics of self-heterodyne to measure comb line linewidth. A Wavelength Selective Switch (WaveShaper) is utilized to filter out individual comb lines from the soliton microcomb into the DSHI setup. The comb line is split into two paths through a beam splitter, with one path passing through an Acoustic Optical Modulator (AOM) for frequency shifting and the other path through a 10-kilometer-long optical fiber delay line. They are then mixed in a photodetector to generate a beatnote containing the phase fluctuation of the comb line. Fig. 2(c) shows the single-sideband (SSB) frequency noise spectra measured at the 1552 nm comb line and the 1542.4 nm comb line, with white noise floors at $17.51 \text{ Hz}^2/\text{Hz}$ and $84.42 \text{ Hz}^2/\text{Hz}$ respectively. Taking into account the relationship between frequency noise (S_ν) and the fundamental linewidth ($\Delta\nu_{ST}$) ($\Delta\nu_{ST}=2\pi S_\nu$), the Lorentzian linewidth of the 1552 nm comb line can be calculated as 107 Hz. The linewidths of the respective comb lines from $m = -21$ to $m = 15$ are shown in Fig. 2(d), following a quadratic pattern as projected by repetition noise[35]. A noise degradation of more than two orders of magnitude can be observed in marginal comb lines, which can impact the communication performance under conventional modulation schemes. Despite that, experimental results indicate that the linewidth of the integrated microcavity OFC is about three orders of magnitude smaller than the linewidth of the

ITLA laser array used in commercial WDM systems[40]. This substantial reduction in linewidth is highly advantageous for long-distance transmission and the implementation of higher-order modulation formats.

3. HIGH-CAPACITY COMMUNICATION SYSTEM BASED ON THE SINGLE SOLITON MICROCOMB

A. Experimental setup

After generating a single soliton microcomb using an integrated microcavity, we construct an OFC coherent communication system to simulate a realistic WDM coherent optical communication scenario. The experimental setup shown in Fig. 3 is used to assess the communication capability of each comb tooth in the soliton microcomb, which implements adaptive modulation and bandwidth allocation strategies. To simulate typical WDM communication transmission scenarios, the OFC is divided into odd and even carrier groups using a WDM multiplexer. A C-band programmable filter (Finisar WaveShaper) is used to function as the WDM multiplexer. Following this, each set of odd and even carriers is amplified separately using polarization-maintaining EDFAs before being modulated by two IQMs. Since only one DP-IQM is available, the amplified even optical carriers are injected into an IQM for modulation. To simulate the dual-polarization modulation, the output of the modulator is divided into two branches by an optical coupler (OC), with both branches theoretically having equal power. As shown in Fig. 3, to achieve de-correlation between the two branches, a delay line of about 1 meter is added to the lower branch in order to introduce an appropriate time delay. This delay ensures that the two channels are sufficiently differentiated to form a doubly polarized signal when merged via the OC.

After modulating the odd and even carriers, the signals are

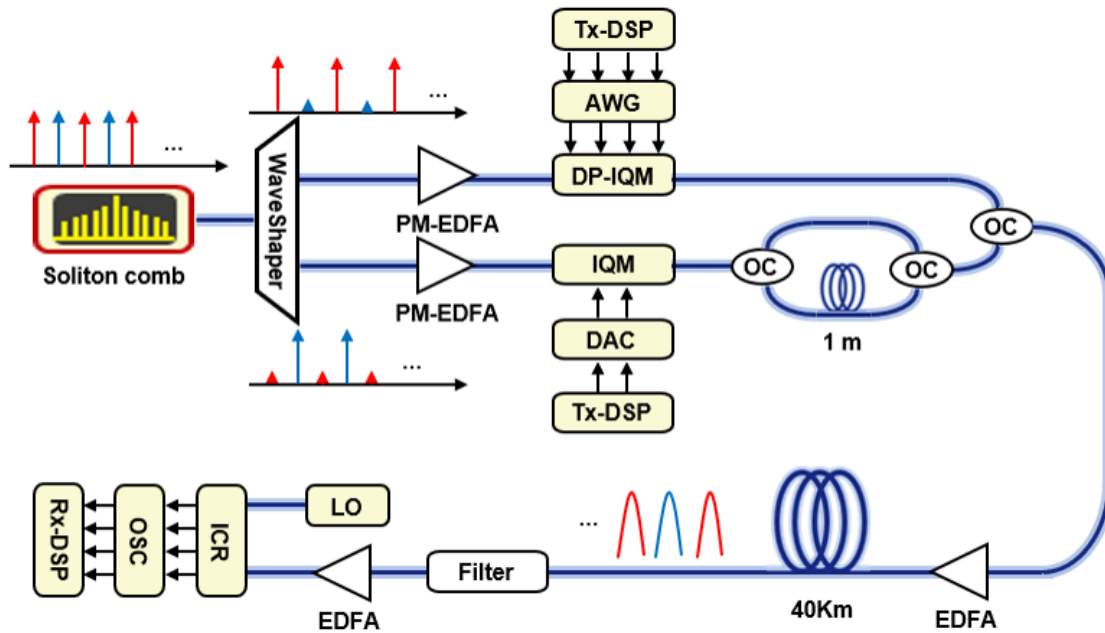


Fig. 3. Experimental setup for soliton microcomb coherent communication. WaveShaper: Waveform Shaper; Tx-DSP: Data Signal Processing Send Port; AWG: Arbitrary Waveform Generator; DAC: Digital to Analog Converter; DP-IQM: Dual Polarization IQM; OC: Optical Coupler; Fiber: 40 km of Single Mode Fiber; PM-EDFA: Bias-Preserving Erbium-Doped Fiber Amplifier; Filter: narrow-band optical filter; ICR: coherent optical receiver; OSC: real-time oscilloscope; Rx-DSP: data signal processing receiver port; and LO: Local Oscillator.

combined using an OC combiner, and Fig. 4(a) depicts the spectrum of the resultant signal. Prior to transmission through a 40-kilometer single-mode fiber, the modulated signal is further amplified by an EDFA. At the receiver end, the signal is filtered through a narrowband optical filter with a bandwidth of 75 GHz. The filtered single-channel signal is then directed to the coherent receiver for demodulation by the Local Oscillator (LO) and captured by the real-time oscilloscope (OSC). The drive signals for the DP-IQM and the IQM are generated by a four-channel Arbitrary Waveform Generator (AWG) at 64 GS/s and a two-channel Digital-to-Analog Converter (DAC) at 80 GS/s, respectively. Importantly, the bias point of the Mach-Zehnder modulator (MZM) is deliberately adjusted closer to its null point to reduce optical fluctuations in the waveform's lower region. For modulation, Quadrature Phase Shift Keying (QPSK) or 16-Quadrature Amplitude Modulation (16QAM) formats are used, combined with cosine-shaped raised cosine pulse shaping, with a roll-off factor (β) at 0.1.

B. Experimental results

Due to the strong attenuation of the C-band waveform shaper at the edge of the band, modulation and capacity measurements are performed only on 39 comb line with wavelengths ranging from 1532 nm to 1562.4 nm at a wavelength spacing of approximately 0.8 nm, as determined by the comb FSR. Fig. 4(a) displays the optical spectra of the 39 modulated optical combs using 40Gbaud 16QAM signals. Notably, due to the low OSNR and large frequency noise of the 12 combs in the C-band soliton microcombs with wavelengths lower than 1541.6 nm, error-free transmission is not possible using 40Gbaud and 16QAM, so 40Gbaud and QPSK modulation are used to measure the BER. The BER of

each channel after demodulation is shown in Fig. 4(b). The results reveal significant variations in communication capabilities among different combs of the same soliton microcomb. If the same modulation format and symbol rate are used across all combs, the overall communication performance is limited by the poorest-performing comb, known as the "barrel effect". Therefore, selecting an appropriate modulation scheme for each comb line is crucial for microcomb-based communication.

To more accurately and reliably investigate the relationship between the communication performance of soliton microcombs and OSNR, the data of the three comb lines that are affected by the ASE noise from the EDFA are ignored, retaining only the data of the pump light with the same baseline noise. The blue dots in Fig. 4(c) are the relationship between BER and OSNR for the 9 channels from 1541.6nm to 1548nm with 40Gbaud 16QAM, while red dots are the 12 channels from 1532nm to 1540.8nm using the 40Gbaud QPSK. The experimental results for both modulation formats show that the BER increases with the decrease of the OSNR, causing the degradation of the communication performance. Although increasing the optical pump power can improve the OSNR of the soliton microcombs and enhance overall communication performance, this approach is power consuming and does not address the uneven OSNR distribution of the soliton microcombs fundamentally. It is noteworthy that the 6 channels from 1539.2 nm to 1543.2 nm have similar OSNRs, yet the 3 channels from 1539.2 nm to 1540.8 nm cannot achieve error-free transmission with the 40 Gbaud 16QAM as effectively as the channels from 1541.6 nm to 1543.2 nm. This indicates that OSNR is not the sole factor influencing OFC communication performance. The increasing linewidth of the comb lines from 1543.2 nm to 1539.2 nm, as shown in Fig. 4(d), reduces constel-

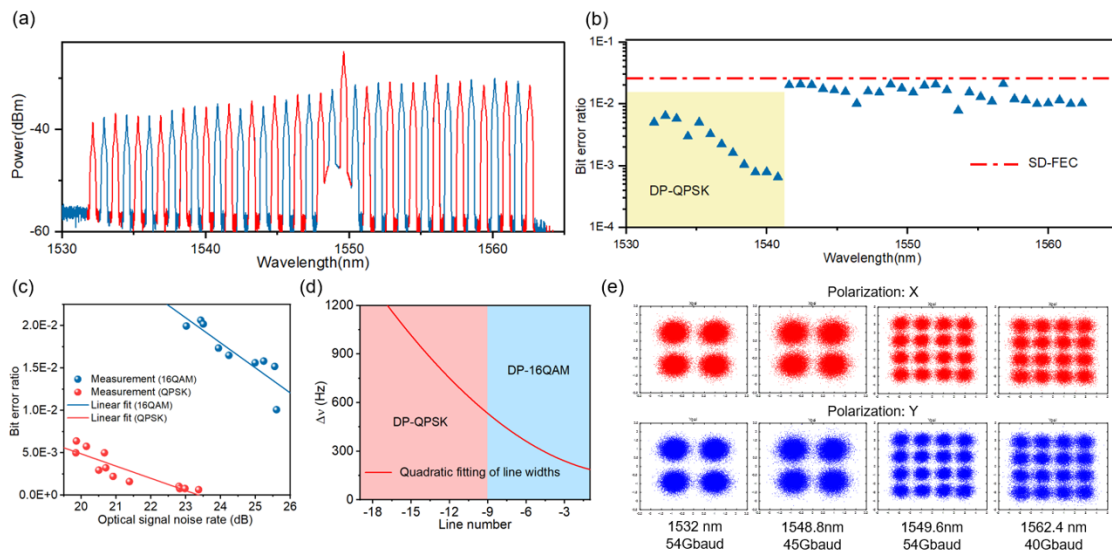


Fig. 4. (a) Optical spectra of 39 channels modulated with 40Gbaud and DP-16QAM modulation format (measured at OC). The red and blue colors of the carriers represent the parity carriers. (b) Measured bit error ratios of the transmitted channels for the single-comb with a received power of -14dBm and a modulation symbol transmission rate of 40Gbaud. The red dashed line indicates the Soft Decision Forward Error Correction (SD-FEC) BER threshold with an overhead of 20%. The 12 lines at the high-frequency edge of the C band (yellow region) are modulated with quadrature phase-shift keying (QPSK) signals rather than 16QAM owing to the large linewidths of these carriers. (c) Measured bit error ratios versus combs OSNR for QPSK modulated channels and neighboring 16QAM modulated channels. (d) The linewidth distribution of the corresponding channel in Fig. c, and the powder blue color of the background represents the modulation formats DP-QPSK and DP-16QAM used by the carriers in range. (e) Constellation diagrams of soliton coherent communication obtained at carrier wavelengths of 1532, 1548.8, 1549.6 and 1562.4 nm at a received power of -14 dBm.

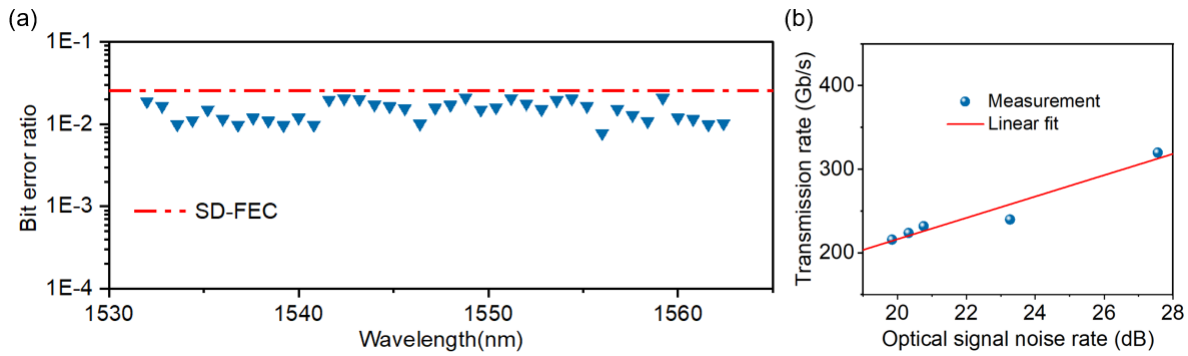


Fig. 5. (a) Measured bit error ratios of the transmitted channels for each channel at the maximum transmission rate with a received power of -14dBm. The red dashed line indicates the Soft Decision Forward Error Correction (SD-FEC) BER threshold with an overhead of 20%. (b) Measured single-wave maximum rate versus OFC OSNR.

297 lation density in phase space, leading to constellation aliasing
 298 and higher BERs. Fig. 4(e) shows the constellation diagrams for
 299 the 1532 nm channel (leftmost C-band), the 1548.8 nm channel
 300 with QPSK modulation due to ASE noise, the 1549.6 nm channel
 301 (pumped light), and the 1562.4 nm channel (rightmost C-band).
 302 These diagrams illustrate the significant impact of ASE noise
 303 on communication performance. Despite channel 1548.8 nm
 304 having a lower capacity than channel 1532 nm, its constellation
 305 diagrams are blurrier. The constellation diagrams indicate good
 306 communication performance across all channels. As shown in
 307 Fig. 4(b), we observe that the optical combs to the left of the
 308 pump light (i.e., those with shorter wavelengths than the pump
 309 light) exhibit a decreasing OSNR and an increasing linewidth
 310 as the wavelength decreases. This combination results in deteri-
 311 orating communication performance for the optical combs on the
 312 left as the wavelength decreases. Conversely, the comb lines
 313 on the right side of the pump light show a more balanced com-
 314 munication performance due to a simultaneous increase in both
 315 OSNR and linewidth. Given these distribution characteristics,
 316 we can employ low-order modulation formats such as QPSK
 317 with higher symbol transmission rates for the optical combs
 318 on the left side of the pump light. For the optical combs on
 319 the right side, which have better communication performance,
 320 higher-order modulation formats such as 16QAM are suitable.
 321 Additionally, when designing the appropriate communication
 322 scheme for each optical comb, it is essential to consider not only
 323 the OSNR and linewidth but also the channel bandwidth to
 324 avoid spectral aliasing.

325 To maximize the transmission rate of soliton microcombs, we
 326 employ adaptive modulation and bandwidth allocation strategies
 327 for the first time in OFC communication systems. Based
 328 on the OSNR and linewidth of different channels, the modula-
 329 tion format and symbol transmission rate are manually adjusted
 330 within the constraint of channel bandwidth until the BER reaches
 331 the threshold of 2.5×10^{-2} defined by the third-generation soft
 332 decision forward error correction (FEC). This approach maxi-
 333 mizes the communication performance of the entire soliton com-
 334 munication system and achieves the highest spectral efficiency.
 335 Using this setup, we determine that the maximum total capacity
 336 of the C-band soliton microcomb to be 10.68 Tbps for the 39 comb
 337 lines. In the wavelength range of 1532 nm to 1540.8 nm, 12 chan-
 338 nels used the QPSK modulation format with baud rates ranging
 339 from 54 Gbaud to 60 Gbaud. This method increases the spec-
 340 tral efficiency from 1.6 bit/s/Hz in the first experiment to 2.31
 341 bit/s/Hz, reflecting a 44.58% improvement, which demonstrates

342 the method's efficacy. Fig. 5(a) shows the transmission BER
 343 measurements for each channel at a received power of -14 dBm
 344 after applying the adaptive modulation and bandwidth alloca-
 345 tion strategy, indicating that each comb achieves near-maximum
 346 communication performance. Fig. 5(b) plots the maximum
 347 communication capacity of the comb versus the OSNR of the comb,
 348 showing a clear linear relationship where higher OSNR allows
 349 for greater data capacity transmission. This result demonstrates
 350 that the original communication performance of soliton micro-
 351 combs can be fully exploited using adaptive modulation and
 352 bandwidth allocation strategies. This is particularly important
 353 for combs with low OSNR and large linewidth, which are often
 354 overlooked because of their poor communication performance.
 355 Given the impending capacity crisis in optical fiber communica-
 356 tion systems, maximizing the communication capacity of each
 357 channel is critical.

358 4. CONCLUSION

359 In summary, we have implemented adaptive modulation and
 360 bandwidth allocation strategies for the first time in a soliton
 361 microcomb communication system. This method employs the
 362 most appropriate capacity-maximizing modulation scheme for
 363 each channel, considering the constraints of channel bandwidth
 364 by detecting the OSNR and linewidth distribution of the soli-
 365 ton microcombs. Furthermore, the method is validated through
 366 two control experiments: the first follows the conventional fixed
 367 modulation scheme, while the second utilizes the method. Our
 368 results indicate that the adaptive modulation and bandwidth
 369 allocation strategy significantly improve the communication per-
 370 formance of soliton microcomb, particularly for the segments of
 371 the comb with initially poor communication performance. Spec-
 372 tral efficiency is improved from 1.6 bit/s/Hz to 2.31 bit/s/Hz,
 373 representing a 44.58% improvement. We evaluate the maximum
 374 communication capacity of the soliton microcombs after 40 km
 375 of transmission, finding that the total communication capacity of
 376 the C-band exceeds 10 Tbps, with the maximum single-channel
 377 rate reaching 432 Gbps. The capacity of the C+L-band is ex-
 378 pected to exceed 20 Tbps. Owing to the simplicity and maturity
 379 of such strategies, they are readily compatible with commercial
 380 components. Our results highlight the potential of integrated
 381 microcavity optical combs as a next-generation light source for
 382 WDM communications, especially in intra/inter-data center net-
 383 works where ultra-low latency and cost-effectiveness are crucial.

384 **Funding.** Natural Science Foundation of Beijing Municipality

(Z210004); National Key Research and Development Program of China (SQ2023YFB2805600); State Key Laboratory of Information Photonics and Optical Communications, BUPT, China (IPOC2021ZT01); Beijing Nova Program from Beijing Municipal Science and Technology Commission (20230484433); Fundamental Research Funds for the Central Universities (2023PY08); Beijing University of Posts and Telecommunications (530224024); National Natural Science Foundation of China (62271517); Basic and Applied Basic Research Foundation of Guangdong Province (2023B1515020003); State Key Laboratory of Advanced Optical Communication Systems and Networks of China (2024GZKF19).

Acknowledgments. The authors thank Bing Duan, Dr. Yongpan Gao and Dr. Huashun Wen for the helpful discussions.

Disclosures. The authors declare no conflict of interest.

Data availability. Data underlying the results presented in this article are not publicly available at this time, but may be obtained from the authors upon reasonable request.

REFERENCES

- N. Froberg, S. Henion, H. Rao, *et al.*, "The ngi onramp test bed: reconfigurable wdm technology for next generation regional access networks," *J. Light. Technol.* **18**, 1697 (2000).
- E. Agrell, M. Karlsson, A. Chraplyvy, *et al.*, "Roadmap of optical communications," *J. optics* **18**, 063002 (2016).
- S. L. Jansen, I. Morita, T. C. Schenk, *et al.*, "Coherent optical 25.8-gb/s ofdm transmission over 4160-km ssmf," *J. Light. Technol.* **26**, 6–15 (2008).
- S. J. Savory, "Digital coherent optical receivers: Algorithms and sub-systems," *IEEE J. selected topics quantum electronics* **16**, 1164–1179 (2010).
- Z. Liu, J.-Y. Kim, D. S. Wu, *et al.*, "Homodyne ofdm with optical injection locking for carrier recovery," *J. Light. Technol.* **33**, 34–41 (2014).
- G. Rademacher, B. J. Puttnam, R. S. Luís, *et al.*, "10.66 peta-bit/s transmission over a 38-core-three-mode fiber," in *optical fiber communication conference*, (Optica Publishing Group, 2020), pp. Th3H–1.
- P. J. Winzer, "Scaling optical fiber networks: Challenges and solutions," *Opt. Photonics News* **26**, 28–35 (2015).
- F. Hamaoka, K. Minoguchi, T. Sasai, *et al.*, "150.3-tb/s ultra-wideband (s, c, and l bands) single-mode fibre transmission over 40-km using >519gb/s/a pdm-128qam signals," in *2018 European Conference on Optical Communication (ECOC)*, (IEEE, 2018), pp. 1–3.
- T. Kobayashi, M. Nakamura, F. Hamaoka, *et al.*, "1-pb/s (32 sdm/46 wdm/768 gb/s) c-band dense sdm transmission over 205.6-km of single-mode heterogeneous multi-core fiber using 96-gbaud pdm-16qam channels," in *2017 Optical Fiber Communications Conference and Exhibition (OFC)*, (IEEE, 2017), pp. 1–3.
- H. Hu, F. Da Ros, M. Pu, *et al.*, "Single-source chip-based frequency comb enabling extreme parallel data transmission," *Nat. Photonics* **12**, 469–473 (2018).
- J. Schröder, A. Fülöp, M. Mazur, *et al.*, "Laser frequency combs for coherent optical communications," *J. Light. Technol.* **37**, 1663–1670 (2019).
- S. A. Diddams, K. Vahala, and T. Udem, "Optical frequency combs: Coherently uniting the electromagnetic spectrum," *Science* **369**, eaay3676 (2020).
- W. Liang, D. Eliyahu, V. S. Ilchenko, *et al.*, "High spectral purity kerr frequency comb radio frequency photonic oscillator," *Nat. communications* **6**, 7957 (2015).
- T. W. Hänsch, "Nobel lecture: passion for precision," *Rev. Mod. Phys.* **78**, 1297–1309 (2006).
- J. Liu, A. S. Raja, M. Karpov, *et al.*, "Ultralow-power chip-based soliton microcombs for photonic integration," *Optica* **5**, 1347–1353 (2018).
- P. Del'Haye, S. A. Diddams, and S. B. Papp, "Laser-machined ultrahigh-q microrod resonators for nonlinear optics," *Appl. Phys. Lett.* **102** (2013).
- S. H. Lee, D. Y. Oh, Q.-F. Yang, *et al.*, "Towards visible soliton micro-comb generation," *Nat. communications* **8**, 1295 (2017).
- G. Frigenti, D. Farnesi, G. Nunzi Conti, and S. Soria, "Nonlinear optics in microspherical resonators," *Micromachines* **11**, 303 (2020).
- D.-Q. Yang, J.-h. Chen, Q.-T. Cao, *et al.*, "Operando monitoring transition dynamics of responsive polymer using optofluidic microcavities," *Light. Sci. & Appl.* **10**, 128 (2021).
- N. Toropov, G. Cabello, M. P. Serrano, *et al.*, "Review of biosensing with whispering-gallery mode lasers," *Light. Sci. & Appl.* **10**, 42 (2021).
- X. Jiang, A. J. Qavi, S. H. Huang, and L. Yang, "Whispering-gallery sensors," *Matter* **3**, 371–392 (2020).
- H. Yang, Z.-G. Hu, Y. Lei, *et al.*, "High-sensitivity air-coupled megahertz-frequency ultrasound detection using on-chip microcavities," *Phys. Rev. Appl.* **18**, 034035 (2022).
- S. A. Diddams, T. Udem, J. Bergquist, *et al.*, "An optical clock based on a single trapped 199hg^+ ion," *Science* **293**, 825–828 (2001).
- Z. L. Newman, V. Maurice, T. Drake, *et al.*, "Architecture for the photonic integration of an optical atomic clock," *Optica* **6**, 680–685 (2019).
- M.-G. Suh, Q.-F. Yang, K. Y. Yang, *et al.*, "Microresonator soliton dual-comb spectroscopy," *Science* **354**, 600–603 (2016).
- P. Trocha, M. Karpov, D. Ganin, *et al.*, "Ultrafast optical ranging using microresonator soliton frequency combs," *Science* **359**, 887–891 (2018).
- J. Riemensberger, A. Lukashchuk, M. Karpov, *et al.*, "Massively parallel coherent laser ranging using a soliton microcomb," *Nature* **581**, 164–170 (2020).
- J. Pfeifle, V. Brasch, M. Lauer, *et al.*, "Coherent terabit communications with microresonator kerr frequency combs," *Nat. photonics* **8**, 375–380 (2014).
- J. Pfeifle, A. Coillet, R. Henriet, *et al.*, "Optimally coherent kerr combs generated with crystalline whispering gallery mode resonators for ultrahigh capacity fiber communications," *Phys. Rev. Lett.* **114**, 093902 (2015).
- P. Marin-Palomo, J. N. Kemal, M. Karpov, *et al.*, "Microresonator-based solitons for massively parallel coherent optical communications," *Nature* **546**, 274–279 (2017).
- Y. Geng, H. Zhou, X. Han, *et al.*, "Coherent optical communications using coherence-cloned kerr soliton microcombs," *Nat. communications* **13**, 1070 (2022).
- T. Salgals, J. Alnis, R. Murnieks, *et al.*, "Demonstration of a fiber optical communication system employing a silica microsphere-based ofc source," *Opt. Express* **29**, 10903–10913 (2021).
- Z. Zhou, J. Wei, Y. Luo, *et al.*, "Communications with guaranteed bandwidth and low latency using frequency-referenced multiplexing," *Nat. Electron.* **6**, 694–702 (2023).
- A. B. Matsko and L. Maleki, "On timing jitter of mode locked kerr frequency combs," *Opt. express* **21**, 28862–28876 (2013).
- F. Lei, Z. Ye, Ó. B. Helgason, *et al.*, "Optical linewidth of soliton microcombs," *Nat. Commun.* **13**, 3161 (2022).
- D. Zou, Y. Chen, F. Li, *et al.*, "Comparison of bit-loading dmt and pre-equalized dft-spread dmt for 2-km optical interconnect system," *J. Light. Technol.* **37**, 2194–2200 (2019).
- W. Wang, Z. Wu, D. Zou, *et al.*, "Training sequences design for simultaneously transceiver iq skew estimation in coherent systems," *J. Light. Technol.* (2024).
- X. Yi, Q.-F. Yang, X. Zhang, *et al.*, "Single-mode dispersive waves and soliton microcomb dynamics," *Nat. communications* **8**, 14869 (2017).
- T. Okoshi, K. Kikuchi, and A. Nakayama, "Novel method for high resolution measurement of laser output spectrum," *Electron. letters* **16**, 630–631 (1980).
- T. Mukaiyama, T. Kimura, and H. Koshi, "Narrow linewidth tunable lasers for digital coherent system," in *2015 Conference on Lasers and Electro-Optics Pacific Rim*, (Optica Publishing Group, 2015), p. 27J1_1.